Annals of Nuclear Medicine Vol. 19, No. 7, 567–572, 2005

Influence of photon scattering and attenuation on ROI analysis in brain perfusion single-photon emission tomographic imaging of normal subjects

Jingming BAI,* Jun HASHIMOTO,* Koichi OGAWA,** Atsushi KUBO,* Atsushi FUKUNAGA,*** Satoshi ONOZUKA*** and Koichi Uchida***

*Department of Radiology, School of Medicine, Keio University
**Department of Electrical Engineering, College of Engineering, Hosei University
***Department of Neurosurgery, School of Medicine, Keio University

Objective: The aim of this study was to evaluate the effect of scatter and attenuation correction in region of interest (ROI) analysis in brain perfusion single-photon emission tomography (SPECT) and to assess the influence of selecting the reference area on semi-quantification. ***Methods:*** Ten normal subjects were enrolled and injected with ^{123}I-iodoamphetamine to undergo simultaneous emission and transmission scanning for scatter and attenuation correction. We reconstructed three SPECT images from common projection data of each subject: with scatter correction and nonuniform attenuation correction, with scatter correction and uniform attenuation correction, and with uniform attenuation correction applied to data without scatter correction. A program for automated ROI drawing was used to set ROIs on various regions in brain images. Regional count ratios were compared in images with different correction procedures by using three different reference areas. ***Results:*** The effect of the combination of scatter and attenuation correction was marked in the precentral, temporal, posterior, hippocampus and especially in the cerebellum. In contrast, it was not appreciable in the central and parietal areas. When using the cerebellar ROI as the reference, the count ratio varied widely depending on the correction procedures. On the other hand, the whole brain reference offered the least variation in the count ratio. ***Conclusions:*** The influence of photon scattering and attenuation was dependent on regions. Since the count in the cerebellar ROI is greatly affected by photon scattering and attenuation, nonuniform attenuation correction combined with scatter correction deserves consideration when using the cerebellar ROI as the reference.

Key words: brain perfusion, brain SPECT, scatter correction, attenuation correction, transmission CT

INTRODUCTION

BRAIN PERFUSION single-photon emission tomography (SPECT) permits not only visual interpretation of images but also quantitative measurement of regional cerebral blood flow. A number of investigators have pointed out that the accuracy of SPECT quantification is degraded by photon scattering and attenuation, and various methods have been reported for scatter and attenuation correction to improve the accuracy.[1–15] Some authors have implemented gamma-ray transmission CT scanning to obtain the attenuation coefficient map, and simultaneous acquisition of emission and transmission data allows no misregistration between SPECT images and the attenuation map.

There are some reports describing the effects of scatter correction,[10,11,15] attenuation correction[7,13] and both[5] on brain perfusion imaging in normal subjects. However, no article has focused on the influence of photon scattering and attenuation on regions of interest (ROI) analysis employing a specific reference area and calculating regional count ratios to the reference area, although ROI analysis is the most popular method for quantification

Received May 10, 2005, revision accepted July 14, 2005.

For reprint contact: Jun Hashimoto, M.D., Department of Radiology, School of Medicine, Keio University, 35 Shinanomachi, Shinjuku-ku, Tokyo 160–8582, JAPAN.

This study was not financially supported by any institution or company.

E-mail: junhashi@rad.med.keio.ac.jp

when not measuring absolute values of regional cerebral blood flow. In the analysis, it is important to consider the problem of interobserver difference in ROI setting to assess the significance of scatter and attenuation correction.

In the current study, we evaluated the positional dependence of the effect of scatter and attenuation correction in ROI analysis and also assessed the influence of selecting the reference area on semi-quantification. To overcome the possible misregistration, we reconstructed SPECT images of each subject with different correction procedures by using a common projection data obtained with simultaneous emission and transmission scanning and processed with common slicing. Moreover, to eliminate the problem of interobserver difference in ROI setting, we used a software which permits completely automatic and objective ROI setting.

MATERIALS AND METHODS

Subjects

The present study enrolled ten subjects meeting all of the following criteria: absence of any history of neurological diseases, no signs of neurological disorders on physical

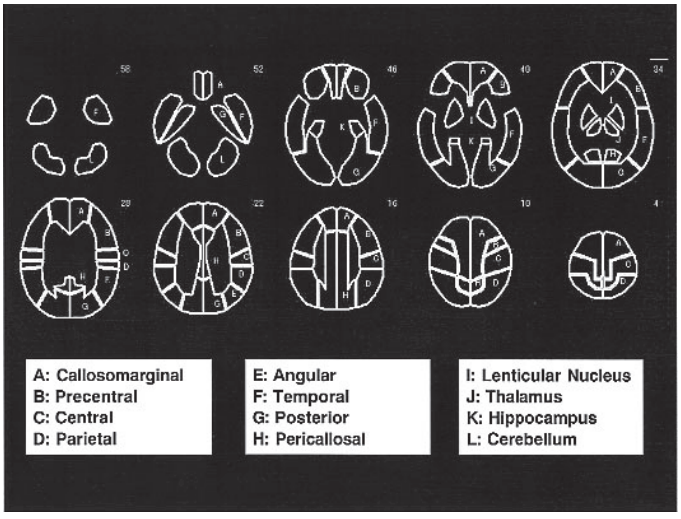

Fig. 1 Automated ROI setting.

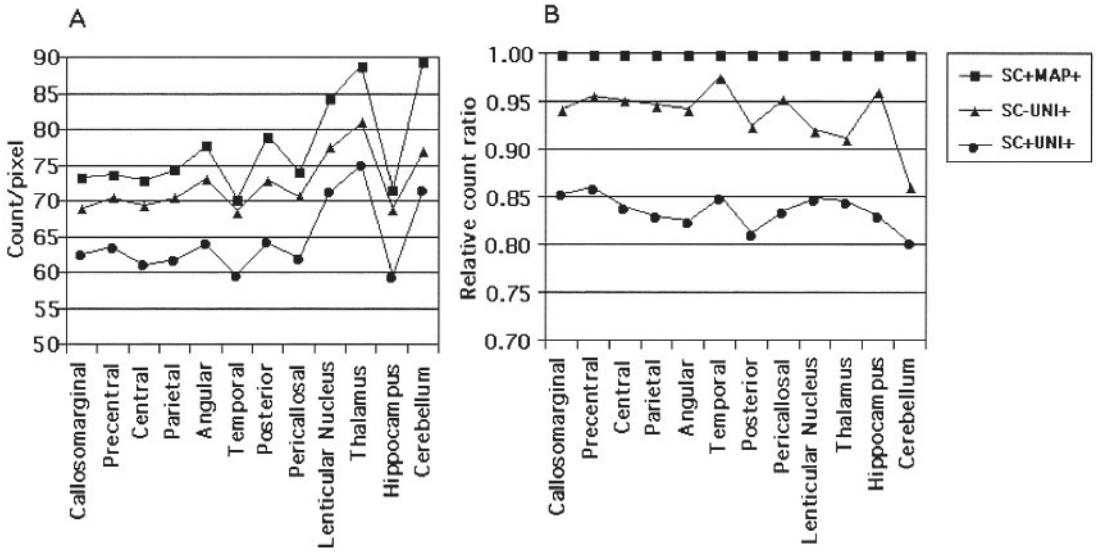

Fig. 2 Regional ROI counts (A) and relative count ratios (B) in images obtained with three different correction methods. SC: scatter correction; MAP: nonuniform attenuation correction; UNI: uniform attenuation correction; +: with correction; –: without correction. In panel B, relative count ratios were calculated by standardizing regional ROI counts with counts in images with scatter correction and nonuniform attenuation correction.

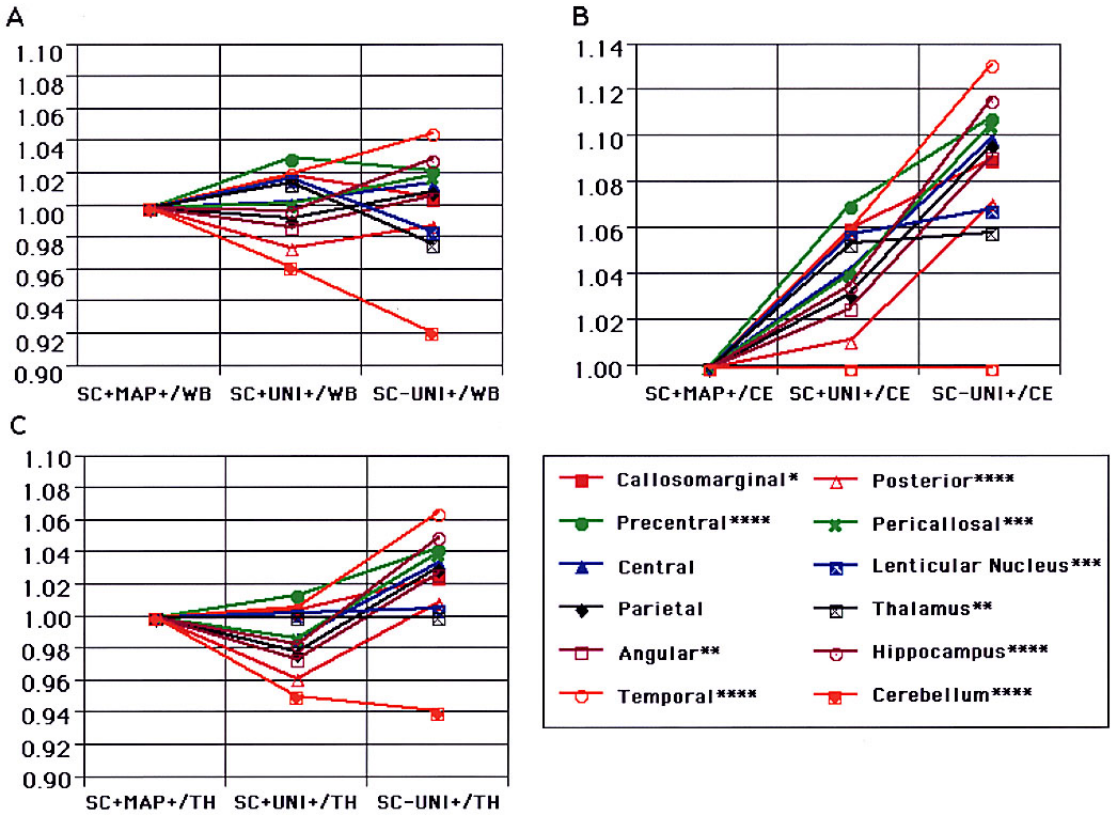

Fig. 3 Effect of scatter and attenuation correction, and influence of selection of reference area on count ratios in ROI analysis. The figure shows relative values of count ratios obtained as follows. First, the regional count ratio was calculated by dividing the mean ROI count in each region by the mean count in the reference ROI. The whole brain (A), cerebellum (B) and thalamus (C) were selected as the reference. Then, the count ratios in images generated with different correction methods were standardized by the count ratio of each region in the image with scatter correction and nonuniform attenuation correction. Further information is provided in the result section of the text. SC: scatter correction; UNI: uniform attenuation correction; MAP: nonuniform attenuation correction; +: with correction; −: without correction; WB: whole brain reference; CE: cerebellar reference; TH: thalamic reference. *: $p < 0.05$; **: $p < 0.01$; ***: $p < 0.001$; ****$p < 0.0001$ (comparison of count ratios obtained with three different correction procedures by using repeated ANOVA)

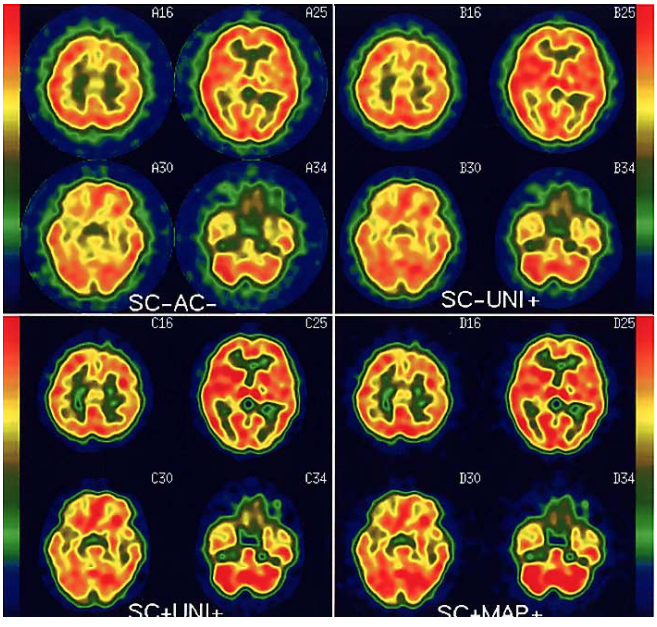

Fig. 4 Transaxial SPECT images of one normal subject. SC: scatter correction; AC: attenuation correction; UNI: uniform attenuation correction; MAP: nonuniform attenuation correction; −: without correction; +: with correction.

examination, no remarkable abnormalities in brain MRI, and no remarkable hypoperfused areas in visual interpretation of brain perfusion SPECT. Written informed consent was obtained after detailed explanation of the study protocol. This study was conducted according to the governmental and institutional regulations for protection of data privacy and confidentiality.

Instrumentation and data acquisition

Subjects were injected with 222 MBq of *N*-isopropyl-4-[^{123}I]iodoamphetamine (^{123}I-IMP) (Nihon Medi-Physics, Tokyo). SPECT data were acquired from 23 minutes to 57 minutes after the administration.

All images in this investigation were obtained with a three-headed rotating camera system equipped with fan-beam collimators (GCA-9300A/DI, Toshiba Corporation, Tokyo) and processed with a medical image processor (GMS-5500 A/DI, Toshiba Corporation, Tokyo). Methods for data acquisition and image processing are the same as those we have previously reported.[8] Transmission and emission projection data were simultaneously acquired by using a ^{99m}Tc external source and four energy windows: (a) 126–133 keV, (b) 134–144 keV, (c) 145–176 keV and (d) 177–187 keV. This combination of the external source and window setting enables us to obtain pure TCT data without scattered photons and scatter-corrected ECT data with one scan.[8]

Image processing

After SPECT imaging with 360 degrees rotation of each gamma camera, one camera opposite the external source acquires emission and transmission data and the other two acquire only emission data because the fan-beam collimators reject almost all of the photons emitted from the external source and scattered in the body.[4,8] For emission data, scatter correction was conducted with the TEW (triple-energy window) method applied to the averaged emission data of the two cameras in windows (b) as the lower subwindow, (c) as the main window and (d) as the upper subwindow.[1,2,8] In the data of the camera opposite the external source, transmission projection data were separated by subtracting the averaged projection data measured by the other two cameras at each view angle.

Separated transmission data were reconstructed to a map of attenuation coefficients. This attenuation map for ^{99m}Tc was converted to that for ^{123}I by multiplying a factor of 0.98.[8] For attenuation correction we used a correction matrix method,[16] which is a modified version of Chang's iterative method. One iteration was performed.

Emission data were reconstructed into a 128 × 128 matrix by the filtered backprojection method with a ramp filter to obtain 3.44 mm-interval transaxial SPECT images. After using a pre-processing filter (Butterworth, order 8, cut-off: 0.10 cycles/pixel), SPECT images with the following three combinations of correction were generated: with scatter correction and attenuation correction using the above attenuation map, with scatter correction and attenuation correction assuming a uniform attenuation coefficient of 0.146 (1/cm), without scatter correction and with attenuation correction assuming a uniform attenuation coefficient of 0.09 (1/cm). The former uniform attenuation coefficient is the theoretical value for water and the latter is the broad μ value determined by a phantom experiment. The map for uniform attenuation correction includes the same μ value in all the pixels within the head contour of each subject. The contour was delineated after seeking an appropriate count threshold in each reconstructed image.

Image analysis

Regions of interest were drawn by three-dimensional stereotaxic ROI template (3DSRT) program.[17] This program allows fully automatic and objective ROI setting by incorporating anatomical standardization of SPECT images based on the statistical parametric mapping (SPM) program,[18,19] and computerized ROI placing on the above standardized SPECT images. The program employs 536 ROIs, which were grouped into 24 regions for data analysis as indicated in Figure 1.

The count ratio for each ROI (mean count in a ROI/mean count in the reference area) was calculated with the following three different reference areas: the whole brain, cerebellum and thalamus. The whole brain count was obtained by averaging counts in all 536 ROIs. The count ratios in the right and left sides were averaged in the same area, which means that 12 ratios were obtained for one reference area in each subject. This calculation was conducted on SPECT images of three different combinations of scatter and attenuation correction as described in the previous section.

Statistics

To compare the effect of scatter and attenuation correction in each area, repeated ANOVA (Stat View ver.4.5, Abacus Concepts, Inc., Berkeley) was employed for statistical analysis. A p value < 0.05 was considered statistically significant.

RESULTS

Figure 2 shows regional ROI counts and count ratios in images obtained with three different correction methods. Data of ten subjects were averaged. Panel A includes raw count data (count/pixel). In all correction methods, counts in lenticular nuclei, thalamus and cerebellum were higher than those in other areas. Panel B indicates count data standardized by the count of each region in the image with scatter correction and transmission scan-based attenuation correction. Scatter corrected data with uniform attenuation correction showed the lowest counts followed by images with uniform attenuation correction applied to data without scatter correction. Effect of map-based at-

tenuation correction was most appreciable in the cerebellum and posterior compared with that of uniform correction (comparing the SC+MAP+ and SC+UNI+ lines). Scatter correction yielded marked count reduction especially in the angular, temporal, posterior and hippocampal ROIs (comparing the SC−UNI+ and SC+UNI+ lines).

Figure 3 shows relative values of count ratios calculated by using three different reference areas and standardized by the count ratio of each region in the images with scatter correction and transmission scan-based attenuation correction. The statistical analysis indicates that the effect of combination of scatter and attenuation correction was marked in the precentral, temporal, posterior, hippocampus and especially in the cerebellum. In contrast, it was not appreciable in the central and parietal areas. When using the cerebellar ROI as the reference (Panel B), overestimation of the regional count ratio ranged from 6% to 13% in images without scatter correction and with uniform attenuation correction. In contrast, the whole brain reference (Panel A) yielded overestimation or underestimation of count ratios less than 5% except the cerebellar region manifesting underestimation of 8% in images without scatter correction but with uniform attenuation correction.

Figure 4 includes reconstructed SPECT images and the attenuation coefficient map obtained from one subject. In the visual image interpretation, when comparing the upper two panels, attenuation correction provided relatively increased uptake in the lenticular nucleus, thalamus, brain stem and inner parts of the temporal and occipital lobes. In comparison between the upper right and lower left panels, relatively increased uptake was observed in the lenticular nucleus, thalamus, brain stem and cerebellum after scatter correction. Moreover, contrast between cortex and white matter was augmented by scatter correction. Slightly increased uptake in the cerebellum, occipital and the posterior part of the temporal lobe after nonuniform attenuation correction can be recognized by comparing the lower two panels.

DISCUSSION

We have previously reported the accuracy and feasibility of the method for scatter and attenuation correction incorporating a simultaneous ^{123}I emission and ^{99m}Tc transmission scan that was used in the present study.[8] According to the results of the phantom experiment performed in the above study, SPECT measurement of absolute activity was quite accurate with smaller amounts of error than quantification using images with uniform attenuation correction or without scatter correction. On the basis of the results, we chose to use the images with scatter correction and transmission scan-based attenuation correction as the standard in comparing images obtained with other methods for correction.

In SPECT semi-quantification without measuring absolute values of regional cerebral blood flow, the cerebellum is typically used for reference to calculate relative count ratios. The present study showed that the count in the cerebellar ROI is most susceptible to photon scattering and attenuation among all areas. The most important reason accounting for this phenomenon is that the cerebellum is surrounded by thick bones attenuating and scattering photons.[11,14,15] In addition, head rest is situated near the cerebellum. Rajeevan et al. reported that attenuation correction including the head-holder increased the occipital ROI counts by about 2% compared with correction without considering the influence of the head-holder.[7] Therefore, scatter correction and nonuniform attenuation correction deserve consideration when using the cerebellum as the reference area.

If transmission scan-based attenuation correction or scatter correction is not available, the whole brain seems to be suitable as the reference rather than the cerebellum in the absence of cerebral infarction of a certain amount. The reference of the thalamic ROI also provides a relatively small effect of photon scattering and attenuation (Fig. 3); however thalamus is susceptible to infarction or hemorrhage, and its structure is small, which may lead to instability of the ROI analysis. Another conceivable substitute to evaluate the severity of reduced perfusion is the use of the statistical mapping incorporating transformation to the standard brain and comparison with normal files.[18,19] When the normal file and the patient's data are generated with the same correction method (even though transmission scan-based attenuation correction is not implemented), some of the systematic influences of photon scattering and attenuation are expected to be reduced in statistical comparison. However, the disadvantage of the method is the need for constructing a normal database.

The current study showed the region-dependent effect of scatter and attenuation correction in ROI analysis of brain perfusion SPECT. According to the results of the statistical analysis indicated in Figure 3, when using whole brain as the reference, the effect of the combination of scatter and attenuation correction was most marked in the precentral, temporal, posterior, hippocampus and cerebellum. In contrast, the effect of correction was not appreciable in ROIs drawn on the central and parietal areas.

Regarding the comparison between uniform and nonuniform attenuation corrections, areas near effective attenuators including bones gain more counts than other areas after inhomogeneous attenuation correction. The results indicated in Figure 3 suggest that the cerebellar and posterior count ratios after nonuniform attenuation correction are higher than those after uniform correction because of the influence of the adjacent bones and the head rest as mentioned above. In contrast, regions near air spaces gain relatively small counts after inhomogeneous attenuation correction. Figure 3 also shows that the precentral area yielded relatively higher count ratios under

uniform attenuation correction probably because the lower parts of the area are located near the air spaces of nasal and paranasal cavities (Fig. 1).

The effect of scatter correction also varied depending on the region. The count ratios in the temporal and hippocampus markedly decreased after scatter correction (Fig. 3) because of the higher amount of scatter fraction there than in other areas. These structures are adjacent to the occipital lobe or the temporal-occipital associated area including higher amount of the tracer. The markedly decreased count ratios after scatter correction in the temporal and hippocampal areas seem to be attributable to the exclusion of scattered photons emitted from the adjacent areas. The influence of scattered photons in the above regions should be considered in diagnosing Alzheimer's disease often affecting the sites. On the other hand, the cerebellum, lenticular nucleus and thalamus offered relatively higher count ratios after scatter correction because of the lower amount of scatter fraction in images without correction. These areas contain higher counts than other areas and are not surrounded by structures manifesting high counts, which offer a lower scatter fraction.

In summary, we assessed the effect of scatter and attenuation correction in ROI analysis in brain perfusion SPECT of normal subjects and elucidated the influence of selecting the reference area on semi-quantification. The effect varied depending on the anatomical position. Use of the cerebellar reference resulted in varied count ratios depending on correction procedures; in contrast, the whole brain reference entailed stable calculation. Nonuniform attenuation correction combined with scatter correction warrants implementation when using the cerebellar ROI as the reference. Further investigations are required enrolling patients with neurological diseases.

REFERENCES

1. Ogawa K, Harata Y, Ichihara T, Kubo A, Hashimoto S. A practical method for position-dependent Compton-scatter correction in single photon emission CT. *IEEE Trans Med Imag* 1993; 10: 408–412.
2. Ichihara T, Ogawa K, Motomura N, Kubo A, Hashimoto S. Compton scatter correction using triple-energy window method for single- and dual-isotope SPECT. *J Nucl Med* 1993; 34: 2216–2221.
3. Meikle SR, Hutton BF, Bailey DL. A transmission-dependent method for scatter correction in SPECT. *J Nucl Med* 1994; 35: 360–367.
4. Hashimoto J, Kubo A, Ogawa K, Amano T, Fukuuchi Y, Motomura N, et al. Scatter and attenuation correction in technetium-99m brain SPECT. *J Nucl Med* 1997; 38: 157–162.
5. Iida H, Narita Y, Kado H, Kashikura A, Sugawara S, Shoji Y, et al. Effects of scatter and attenuation correction on quantitative assessment of regional cerebral blood flow with SPECT. *J Nucl Med* 1998; 39: 181–189.
6. Stodilka RZ, Kemp BJ, Prato FS, Nicholson RL. Importance of bone attenuation in brain SPECT quantification. *J Nucl Med* 1998; 39: 190–197.
7. Rajeevan N, Zubal IG, Ramsby SQ, Zoghbi SS, Seibyl J, Innis RB. Significance of nonuniform attenuation correction in quantitative brain SPECT imaging. *J Nucl Med* 1998; 39: 1719–1726.
8. Ogasawara K, Hashimoto J, Ogawa K, Kubo A, Motomura N, Hasegawa H, et al. Simultaneous acquisition of iodine-123 emission and technetium-99m transmission data for quantitative brain single photon emission tomographic imaging. *Eur J Nucl Med* 1998; 25: 1537–1544.
9. Hashimoto J, Sasaki T, Ogawa K, Kubo A, Motomura N, Ichihara T, et al. Effects of Scatter and Attenuation Correction on Quantitative Analysis of β-CIT Brain SPECT. *Nucl Med Commun* 1999; 20: 159–165.
10. Licho R, Glick SJ, Xia W, Pan TS, Penney BC, King MA. Attenuation compensation in ^{99m}Tc SPECT brain imaging: a comparison of the use of attenuation maps derived from transmission versus emission data in normal scans. *J Nucl Med* 1999; 40: 456–463.
11. Ito H, Iida H, Kinoshita T, Hatazawa J, Okudera T, Uemura K. Effects of scatter correction on regional distribution of cerebral blood flow using I-123-IMP and SPECT. *Ann Nucl Med* 1999; 13: 331–336.
12. Laere KV, Koole M, Kauppinen T, Monsieurs M, Bouwens L, Dierck R. Nonuniform transmission in brain SPECT using ^{201}Tl, ^{153}Gd, and ^{99m}Tc static line sources: anthropomorphic dosimetry studies and influence on brain quantification. *J Nucl Med* 2000; 41: 2051–2062.
13. Laere KV, Koole M, Versijpt J, Dierckx R. Non-uniform versus uniform attenuation correction in brain perfusion SPECT of healthy volunteers. *Eur J Nucl Med* 2001; 28: 90–98.
14. Kado H, Iida H, Kimura H, Ogawa T, Narita Y, Hatazawa J, et al. Brain perfusion SPECT study with ^{99m}Tc-bicisate: clinical pitfalls and improved diagnostic accuracy with a combination of linearization and scatter-attenuation correction. *Ann Nucl Med* 2001; 15: 123–129.
15. Shiga T, Kubo N, Takano A, Kobayashi J, Takeda Y, Nakamura F, et al. The effect of scatter correction on ^{123}I-IMP brain perfusion SPECT with the triple energy window method in normal subjects using SPM analysis. *Eur J Nucl Med* 2002; 29: 342–345.
16. Ogawa K, Takagi Y, Kubo A, Hashimoto S, Sanmiya T, Okano Y, et al. An attenuation correction method of single photon emission computed tomography using gamma ray transmission CT. *KAKU IGAKU (Jpn J Nucl Med)* 1985; 22: 477–490.
17. Takeuchi R, Yonekura Y, Matsuda H, Konishi J. Usefulness of a three-dimensional stereotaxic ROI template on anatomically standardized ^{99m}Tc-ECD SPECT. *Eur J Nucl Med* 2002; 29: 331–341.
18. Friston KJ, Frith CD, Liddle PF, Frackowiak RSJ. Plastic transformation of PET images. *J Comput Assist Tomogr* 1991; 15: 634–639.
19. Friston KJ, Holmes AP, Worsely KJ, Poline JP, Frith CD, Frackowiak RSJ. Statistical parametric maps in functional imaging: a general linear approach. *Hum Brain Mapping* 1995; 2: 189–210.